JOURNAL OF AGRICULTURAL AND FOOD CHEMISTRY

pubs.acs.org/JAFC Article

Discovery of *N*-Phenylaminomethylthioacetylpyrimidine-2,4-diones as Protoporphyrinogen IX Oxidase Inhibitors through a Reaction Intermediate Derivation Approach

Da-Wei Wang, Lu Liang, Zhi-Yuan Xue, Shu-Yi Yu, Rui-Bo Zhang, Xia Wang, Han Xu, Xin Wen, and Zhen Xi*

Cite This: *J. Agric. Food Chem.* 2021, 69, 4081−4092 Read Online

ACCESS | Metrics & More | Article Recommendations | Supporting Information

ABSTRACT: Protoporphyrinogen oxidase (PPO, EC 1.3.3.4) is an effective target for green herbicide discovery. In this work, we reported the unexpected discovery of a novel series of *N*-phenylaminomethylthioacetylpyrimidine-2,4-diones (**2**−**6**) as promising PPO inhibitors based on investigating the reaction intermediates of our initially designed *N*-phenyluracil thiazolidinone (**1**). An efficient one-pot procedure that gave 41 target compounds in good to high yields was developed. Systematic *Nicotiana tabacum* PPO (NtPPO) inhibitory and herbicidal activity evaluations led to identifying some compounds with improved NtPPO inhibition potency than saflufenacil and good post-emergence herbicidal activity at 37.5−150 g of ai/ha. Among these analogues, ethyl 2-((((2-chloro-4-fluoro-5-(3-methyl-2,6-dioxo-4-(trifluoromethyl)-3,6-dihydropyrimidin-1(2*H*)-yl)phenyl)amino)methyl)thio)acetate (**2c**) (K_i = 11 nM), exhibited excellent weed control at 37.5−150 g of ai/ha and was safe for rice at 150 g of ai/ha, indicating that compound **2c** has the potential to be developed as a new herbicide for weed management in paddy fields. Additionally, our molecular simulation and metabolism studies showed that the side chains of compound **2c** could form a hydrogen-bond-mediated seven-membered ring system; substituting a methyl group at R^1 could reinforce the hydrogen bond of the ring system and reduce the metabolic rate of target compounds *in planta*.

KEYWORDS: *intermolecular hydrogen bond, one-pot procedure, protoporphyrinogen oxidase, reaction intermediate derivation, weed management*

INTRODUCTION

The use of herbicides to decimate weeds in fields is one of the most effective approaches to improving crop quality. A significant objective of herbicide research is developing new molecules with improved performance.[1] Until now, it remains a challenge for agrochemical research to discover new compounds with a broad spectrum of weed control, improved selectivity, and low application rates.[2] Protoporphyrinogen oxidase (PPO, EC 1.3.3.4) is an effective target for green herbicide discovery. It catalyzes the oxidation of non-fluorescent protoporphyrinogen IX to fluorescent and planar protoporphyrin IX.[3,4] In plants, protoporphyrin IX is the precursor of chlorophyll. Under normal conditions, protoporphyrin IX is directly transformed into chlorophyll by magnesium chelatase without leaking out to the cytoplasm.[5,6] Upon inhibition by inhibitors, the PPO activity is down-regulated and the substrate protoporphyrinogen IX will leak out to the cytoplasm; therein, the substrate can be auto-oxidized to the photosensitizer protoporphyrin IX. In the presence of light, photosensitizing protoporphyrin IX can generate a lot of reactive oxygen species, which, in turn, result in photobleaching of the treated plants.[7−9] PPO-inhibiting herbicides possess many attractive characteristics, including low toxicity, low use rate, favorable environmental safety, and wide spectrum of weed control.[10]

The past decade has witnessed significant progress in PPO inhibitors, and more than 30 PPO inhibiting herbicides are currently used to decimate weeds in the field. According to the structural features, these herbicides mainly categorize into *N*-phenyloxadiazolones, *N*-phenyltriazolinones, diphenyl ethers, and *N*-phenylimides.[11] Pyrimidinediones belong to the *N*-phenylimide chemical family, an extremely active subtype of PPO inhibitors. Currently, four pyrimidinedione derivatives, benzfendizone, butafenacil, saflufenacil, and tiafenacil, have been introduced into the market (Figure 1).[12] Benzfendizone was developed by the FMC Corporation in 1998, which was mainly used for post-emergence grass weeds and broadleaf control in orchards. Besides, benzfendizone also acted as a cotton defoliant and potato desiccant.[13] Butafenacil can effectively control many annual and perennial broadleaf weeds in orchards and non-cropped land by the post-emergence application. Saflufenacil was commercialized by BASF in 2009; it shows rapid control of many dicotyledonous weeds by both pre- and post-emergence applications. Besides,

Received: February 6, 2021
Revised: March 18, 2021
Accepted: March 22, 2021
Published: March 31, 2021

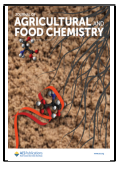

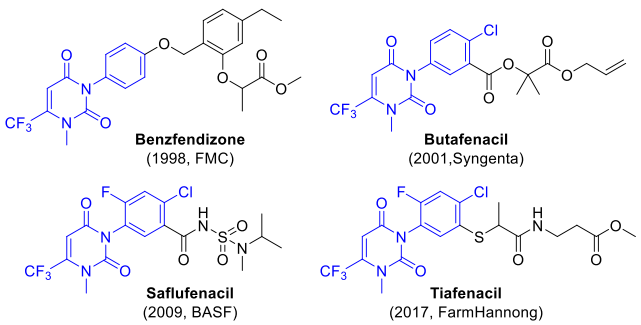

Figure 1. Chemical structures of benzfendizone, butafenacil, saflufenacil, and tiafenacil.

saflufenacil also provides pre-plant burndown against almost all of the major dicotyledonous weeds. Saflufenacil can effectively manage some resistant weeds, such as glyphosate- and AHAS-resistant *Amaranthus* biotypes. Tiafenacil is a relatively new non-selective PPO herbicide developed in 2017 by Farm-Hannong. It has been used together with glyphosate for total vegetation control in orchard and non-till land.

Many studies have suggested that, for the pyrimidinedione derivatives, modification on the 5 position of the benzene ring could affect the physical and chemical properties of target molecules that, in turn, "tune" the bioactivity.[14] To discover new PPO inhibitors, researchers have made enormous efforts to introduce various substituents in this position.[15,16] Among these inhibitors, saflufenacil with fast-acting herbicidal properties is one of the most successful examples. It is proposed that there may be two isomers of saflufenacil: one is an amide form, and another is an imidic acid form. The six-membered ring system of the imidic acid form of saflufenacil can be stabilized by an intramolecular hydrogen-bonding interaction between the hydrogen and oxygen atoms (Figure 2). Therefore, we inferred that installing a ring system at the 5 position of the benzene ring of saflufenacil may be advantageous to bioactivity. Currently, PPO inhibitors are designed by mimicking part of the protoporphyrinogen IX structure,[10] considering that the pyrrole group of protoporphyrinogen IX is a five-membered heterocycle ring. Therefore, we inferred that installing a five-membered ring at this position would accelerate the discovery of new PPO inhibitors. Thiazolidinone is a versatile moiety, and its derivatives possess a diverse array of biological functions, such as antitumor, antidiabetic, anti-inflammatory, and herbicidal activities.[17−20] As a part of our work on exploring potent herbicide candidates, herein, we first present the design and synthesis of *N*-phenyluracil thiazolidinone (**1**) and then report the unexpected discovery *N*-phenylaminomethylthioacetylpyrimidine-2,4-diones (**2−6**) derived from the reaction intermediate of compound **1a1**. Additionally, we also developed an efficient one-pot synthetic method to prepare compounds **2−6**. Systematic herbicidal potency and PPO inhibition activity evaluation of compounds **2−6** resulted in the identification of compound **2c**, a potent and rice-selective herbicide candidate. Besides, to understand the molecular basis, we also performed molecular simulation and metabolism studies on compounds **2c** and **6c**.

MATERIALS AND METHODS

Preparation of Compound 1a1. A solution of 3-(5-amino-4-chloro-2-fluorophenyl)-1-methyl-6-(trifluoromethyl)pyrimidine-2,4-(1*H*,3*H*)-dione (**11a**, 1.0 g), 2-mercaptoacetic acid (0.29 g), HCHO (37% in water, 0.29 g), and *p*-toluenesulfonic acid (25.5 mg) in toluene (100 mL) was heated gradually to reflux with stirring under a nitrogen atmosphere. The water in the reaction system was removed using a Dean−Stark trap. The reaction solution was heated to reflux for 12 h and then cooled to room temperature. Then, 50 mL of saturated $NaHCO_3$ solution was added to the solution; the organic layer was separated; and the water layer was extracted with ethyl acetate (100 mL). The organic layers were combined and washed with saturated NaCl solution (50 mL × 3) and then concentrated. The residue was purified by column chromatography to give light brown solid **1a1** (0.2 g, 16%). ^{1}H NMR (400 MHz, DMSO-d_6): δ 7.93 (d, J = 9.2 Hz, 1H), 7.69 (d, J = 7.2 Hz, 1H), 6.62 (s, 1H), 4.67 (s, 2H), 3.71 (s, 2H), 3.42 (s, 3H). ^{13}C NMR (101 MHz, $CDCl_3$): δ 171.08, 159.54, 158.43, 155.87, 150.32, 141.98, 141.64, 134.83, 134.72, 132.22, 132.19, 131.02, 131.00, 121.64, 121.49, 120.62, 119.07, 118.83, 117.88, 102.99, 102.93, 102.88, 102.82, 48.67, 32.77, 32.73, 32.70, 32.66, 31.74. ^{19}F NMR (376 MHz, $CDCl_3$): δ −65.75

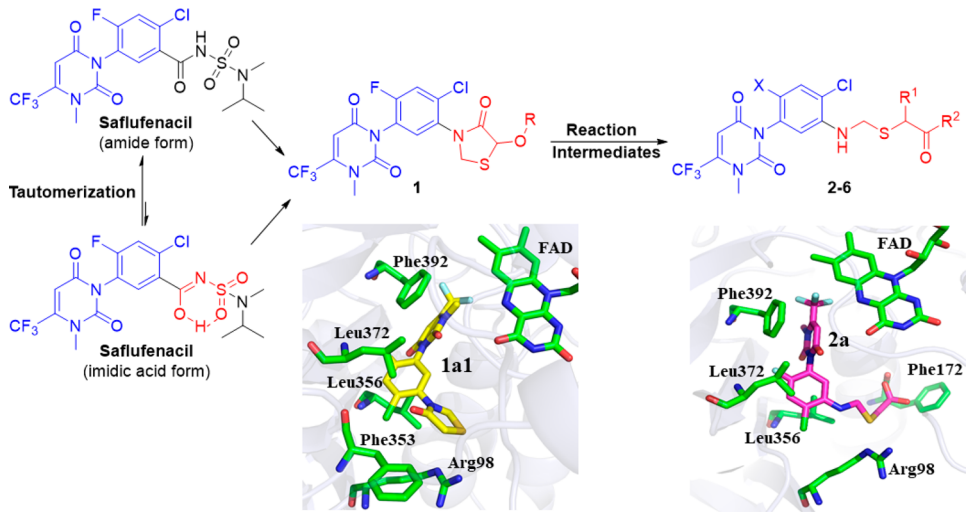

Figure 2. Discovery process of *N*-phenylaminomethylthioacetylpyrimidine-2,4-diones (**2−6**) as PPO inhibitors. The core structures of saflufenacil and compounds **1−6** are shown in blue lines, and the side chains of these compounds are shown in red lines. The docking modes of representative compounds **1a1** and **2a** are shown below compounds **1** and **2−6**, respectively. The structure of compound **1a1** is shown in yellow sticks, the structure of compound **2a** is shown in magenta sticks; and the key residues in the active site are depicted in green sticks.

https://doi.org/10.1021/acs.jafc.1c00796
J. Agric. Food Chem. 2021, 69, 4081−4092

Table 1. Post-emergent Herbicidal Activity, NtPPO Inhibitory Activity, and Calculated *c* Log *P* Values of Compounds 1a1 and 2−5[a]

compound	X	R^1	R^2	yield (%)	dosage (g of ai/ha)	percent inhibition						K_i (nM)	*c* log *P*
						ABUJU	AMARE	ECLPR	DIGSA	ECHCG	SETFA		
1a1				16	150	++++	++++	++++	++++	−	−	3.8	3.88
					75	++++	++++	++++	++++	−	−		
					37.5	++++	++++	++	++	−	−		
2a	F	H	−OH	86	150	++++	++++	++++	++++	+++	++++	11.0	3.62
					75	++++	++++	++++	++++	++	++		
					37.5	++++	++++	+++	+++	+	++		
2b	F	H	$-OCH_3$	92	150	++++	++++	++++	++++	++++	+++	28.6	3.94
					75	++++	++++	++++	+++	+++	+++		
					37.5	++++	++++	++++	++	++	++		
2c	F	H	$-OCH_2CH_3$	86	150	++++	++++	++++	++++	++++	++++	11.0	4.46
					75	++++	++++	++++	++++	++++	++++		
					37.5	++++	++++	++++	++++	++	+++		
2d	F	H	$-OCH_2CH_2CH_3$	85	150	++++	++++	++++	++++	++++	++++	17.4	4.99
					75	++++	++++	++	++	−	++++		
					37.5	+++	++++	+	−	−	++++		
2e	F	H	$-OCH_2CH_2CH_2CH_3$	87	150	++++	++++	++++	+++	+++	+++	15.5	5.52
					75	++++	++++	++++	++	++	++		
					37.5	++++	+++	+++	+	+	+		
2f	F	H	$-(CH_2)_2CH(OCH_3)CH_3$	93	150	++++	++++	++++	++++	+++	+++	8.6	4.69
					75	++++	++++	++++	++++	+	+		
					37.5	++++	++++	+++	++	−	−		
2g	F	H	$-OCH_2CH{=}CH_2$	65	150	++++	++++	++++	++++	++++	++++	37.8	4.71
					75	++++	++++	++++	++	++	++++		
					37.5	++++	++++	−	−	−	+++		
2h	F	H	$-OCH_2C{\equiv}CH$	63	150	++++	++++	+++	++++	++	+++	26.2	4.04
					75	++++	++++	++++	++	−	++		
					37.5	++++	++++	++	−	−	++		
2i	F	H	$-OCH_2CO_2CH_3$	60	150	++++	++++	+++	+++	+++	+++	15.7	3.82
					75	++++	++++	++++	−	−	+++		
					37.5	++++	++++	++	−	−	++		
2j	F	H	$-OCH_2CO_2C_2H_5$	57	150	++++	++++	++++	++++	+++	++++	4.4	4.35
					75	++++	++++	++++	−	−	++++		
					37.5	++++	++++	++	−	−	+		
2k	F	H	$-NHCH_3$	74	150	++++	++++	++++	++++	++	++	27.1	3.08
					75	++++	++++	++	−	−	++		
					37.5	++++	+++	++	−	−	−		
2l	F	H	$-NHCH_2CH_3$	69	150	++++	++++	++++	++	++	++	3.6	3.82
					75	++++	++++	++++	−	−	++		
					37.5	++++	++++	+++	−	−	−		
2m	F	H	$-NHCH_2CH_2CH_3$	73	150	++++	++++	++++	++	++	++	3.0	4.14
					75	++++	++++	++++	−	−	++		
					37.5	++++	+++	+++	−	−	+		
2n	F	H	$-NHCH_2C{\equiv}CH$	56	150	++++	++++	++++	++	+	++	66.8	3.68
					75	++++	++++	++++	−	−	−		
					37.5	++++	++++	++++	−	−	−		
2o	F	H	$-NHCH_2CO_2CH_3$	49	150	++++	++++	++++	++	++	++	47.8	3.37
					75	++++	++++	++++	−	−	+		
					37.5	++++	++++	+++	−	−	−		
2p	F	H	$-NHCH_2CO_2C_2H_5$	48	150	++++	++++	++++	−	++	++	15.3	3.90
					75	++++	++++	++++	−	−	++		
					37.5	+++	++++	++++	−	−	−		
2q	F	H	$-NH(CH_2)_2CO_2CH_3$	50	150	++++	++++	++++	++	−	+++	67.0	3.42
					75	++++	++++	++++	−	−	+		
					37.5	++++	++++	++++	−	−	−		
3a	H	H	−OH	92	150	++	+++	++	−	−	−	46.9	3.46
3b	H	H	$-OCH_3$	86	150	++++	++++	+++	++	++	++	5.1	3.77
3c	H	H	$-OCH_2CH_3$	87	150	++++	++++	+++	−	−	−	6.3	4.30
3d	H	H	$-OCH_2CH_2CH_3$	85	150	++++	++++	++	++	++	++	17.4	4.83

https://doi.org/10.1021/acs.jafc.1c00796
J. Agric. Food Chem. 2021, 69, 4081−4092

Table 1. continued

compound	X	R^1	R^2	yield (%)	dosage (g of ai/ha)	percent inhibition						K_i (nM)	*c* log *P*
						ABUJU	AMARE	ECLPR	DIGSA	ECHCG	SETFA		
3e	H	H	$-OCH_2CH_2CH_2CH_3$	84	150	++++	++++	++	+++	+	−	41.2	5.36
4a	Cl	H	−OH	88	150	−	+	−	−	−	−	38.1	4.19
4b	Cl	H	$-OCH_3$	90	150	++++	++++	+++	+	+	+	6.4	4.51
4c	Cl	H	$-OCH_2CH_3$	85	150	+	+++	+	−	−	−	10.7	5.03
4d	Cl	H	$-OCH_2CH_2CH_3$	88	150	++++	++++	++	++	++	++	11.7	5.56
4e	Cl	H	$-OCH_2CH_2CH_2CH_3$	87	150	+	+++	−	−	−	−	18.9	6.09
5a	Br	H	−OH	83	150	−	−	−	−	−	−	26.9	4.34
5b	Br	H	$-OCH_3$	88	150	−	−	−	−	−	−	10.3	4.66
5c	Br	H	$-OCH_2CH_3$	87	150	−	−	−	−	−	−	13.5	5.18
5d	Br	H	$-OCH_2CH_2CH_3$	86	150	+	++	++	+	+	+	22.4	5.71
5e	Br	H	$-OCH_2CH_2CH_2CH_3$	82	150	−	−	−	−	−	−	23.4	6.24
saflufenacil					150	++++	++++	++++	++++	++++	++++	10.0	4.04
					75	++++	++++	++++	++++	++++	++++		
					37.5	++++	++++	++++	++++	++++	++++		

[a]Abbreviations: ABUJU, *Abutilon juncea*; AMARE, *Amaranthus retroflexus*; ECLPR, *Eclipta prostrata*; DIGSA, *Digitaria sanguinalis*; ECHCG, *Echinochloa crus-galli*; and SETFA, *Setaria faberi*. Rating system for the growth inhibition percentage: ++++, ≥90%; +++, 80−89%; ++, 60−79%; +, 50−59%; and −, <50%.

Table 2. Post-emergent Herbicidal Activity, NtPPO Inhibitory Activity, and Calculated *c* Log *P* Values of Compound 6[a]

compound	X	R^1	R^2	yield (%)	dosage (g of ai/ha)	percent inhibition						K_i (nM)	*c* log *P*
						ABUJU	AMARE	ECLPR	DIGSA	ECHCG	SETFA		
6a	F	$-CH_3$	−OH	76	150	++++	++++	++++	++++	++	++++	14.5	3.93
					75	++++	++++	++++	++	+	++		
					37.5	++++	++++	++++	++	−	++		
6b	F	$-CH_3$	$-OCH_3$	83	150	++++	++++	++++	++++	++++	++++	22.6	4.24
					75	++++	++++	++++	+++	++++	++++		
					37.5	++++	++++	++++	++	+	++		
6c	F	$-CH_3$	$-OCH_2CH_3$	84	150	++++	++++	++++	++++	++++	++++	2.3	4.77
					75	++++	++++	++++	++++	++++	++++		
					37.5	++++	++++	++++	+++	+++	+++		
6d	F	$-CH_3$	$-OCH_2CH_2Cl$	85	150	++++	++++	++++	++++	++++	++++	1.2	4.84
					75	++++	++++	++++	++	++	++		
					37.5	++++	++++	++++	−	−	+		
6e	F	$-CH_3$	$-OCH(CH_3)_2$	82	150	++++	++++	++++	++++	++++	++++	5.6	5.08
					75	++++	++++	++++	++	++	++		
					37.5	++++	++++	++++	−	−	−		
6f	F	$-CH_3$	$-NHCH_3$	67	150	++++	++++	++++	++	−	+++	16.7	3.39
					75	++++	++++	++++	−	−	++		
					37.5	+++	++++	++++	−	−	−		
6g	F	$-CH_3$	$-NHCH_2CH_3$	63	150	++++	++++	++++	++	−	++	2.6	3.92
					75	++++	++++	++++	−	−	+		
					37.5	++++	++++	++++	−	−	−		
6h	F	$-CH_3$	$-NHCH_2CO_2C_2H_5$	49	150	++++	++++	++++	++	−	−	8.5	4.21
					75	++++	++++	++++	−	−	+		
					37.5	++++	++++	++++	−	−	−		
6i	F	$-CH_3$	$-NH(CH_2)_2CO_2CH_3$	48	150	++++	++++	++++	+++	++	++	20.0	4.49
					75	++++	++++	++++	+	−	++		
					37.5	++++	++++	+++	−	−	−		
saflufenacil					150	++++	++++	++++	++++	++++	++++	10.0	4.04
					75	++++	++++	++++	++++	++++	++++		
					37.5	++++	++++	++++	++++	++++	++++		

[a]Abbreviations: ABUJU, *Abutilon juncea*; AMARE, *Amaranthus retroflexus*; ECLPR, *Eclipta prostrata*; DIGSA, *Digitaria sanguinalis*; ECHCG, *Echinochloa crus-galli*; and SETFA, *Setaria faberi*. Rating system for the growth inhibition percentage: ++++, ≥90%; +++, 80−89%; ++, 60−79%; +, 50−59%; and −, <50%.

(s), from −115.35 to −115.58 (m). HRMS (ESI): calculated for $C_{15}H_{10}ClF_4N_3NaO_3S$ $[M + Na]^+$, 445.9965; found, 445.9963.

Synthesis of Compound 2a. A mixture of 3-(5-amino-4-chloro-2-fluorophenyl)-1-methyl-6-(trifluoromethyl)pyrimidine-2,4(1*H*,3*H*)-

https://doi.org/10.1021/acs.jafc.1c00796
J. Agric. Food Chem. 2021, 69, 4081−4092

Table 3. Post-emergence Crop Selectivity of Compounds 2a−2c and 6a−6c and Saflufenacil

		crop injury (%)					
compound	dosage (g of ai/ha)	corn	rice	wheat	soybean	cotton	peanut
2a	150	30	10	70	80	70	85
2b	150	30	50	0	50	50	90
2c	150	40	10	70	95	95	85
6a	150	20	40	80	60	60	60
6b	150	40	40	70	60	70	60
6c	150	50	60	50	60	80	90
saflufenacil	75	50	80	30	80	90	70

dione (**11a**, 0.5 g), 2-mercaptoacetic acid (0.14 g), and paraformaldehyde (89 mg) in toluene (50 mL) was heated to reflux with stirring under a nitrogen atmosphere for 6 h. Then, the reaction solution was cooled to room temperature, and H_2O (20 mL) was added to the reaction solution. The organic layer was separated and washed with H_2O (20 mL) and brine (20 mL × 2), dried by $MgSO_4$, and concentrated by rotary evaporation. The crude compound was purified by column chromatography to give white solid **2a** (0.56 g, 86%). ^{1}H NMR (400 MHz, DMSO-d_6): δ 12.59 (s, 1H), 7.52 (d, J = 9.2 Hz, 1H), 6.92 (d, J = 6.8 Hz, 1H), 6.57 (s, 1H), 6.47 (t, J = 6.8 Hz, 1H), 4.48 (dd, J = 6.4 and 3.2 Hz, 2H), 3.42 (s, 3H), 3.33 (s, 2H). ^{13}C NMR (101 MHz, DMSO-d_6): δ 172.30, 160.44, 150.99, 150.66, 148.26, 141.36, 141.03, 139.94, 139.92, 122.40, 122.26, 119.48, 119.39, 117.47, 117.23, 113.83, 103.25, 46.96, 32.83, 32.21. ^{19}F NMR (376 MHz, $CDCl_3$): δ −65.75 (s), from −114.94 to −115.60 (m). HRMS (ESI): calculated for $C_{15}H_{12}ClF_4N_3NaO_4S$ [M + Na]$^+$, 464.0071; found, 464.0021.

The synthetic details, nuclear magnetic resonance (NMR), and high-resolution mass spectra (HRMS) characterization data of compounds **2b−2q** and **3−6** are shown in the Supporting Information.

NtPPO Inhibitory Activity. In the PPO inhibition assay studies, we selected *Nicotiana tabacum* mitochondrial PPO2 (NtPPO) as the representative plant enzyme because it is widely used as a model enzyme for PPO research.[15,21−23] In this study, the NtPPO expression, purification, and enzyme kinetics assay methods were performed as described previously.[11,24−27] Briefly, in a 96 well plate (Thermo), each well was added 200 μL of the reaction solution. The solution consisted of 200 mM imidazole, 0.03% Tween 80 (v/v), 100 mM potassium phosphate buffer (PBS, pH 7.4), 5 mM dithiothreitol (DTT), 1 mM ethylenediaminetetraacetic acid (EDTA), 0−35 μg of recombinant NtPPO protein, and 0.00001−200 μM inhibitors. The enzymatic reaction was initiated by adding 0.5−3 μM protoporphyrinogen IX. After 0.5−3 μM protoporphyrinogen IX was added to the reaction solution to initiate the enzymatic catalytic reaction, the fluorescent intensity of each well was recorded at the emission wavelength of 630 nm under excitation at 410 nm. The inhibition constant of the enzymatic reaction (K_i) of each compound was calculated by the method reported by Shepherd and Dailey[28] For each compound, three repeats were performed independently, and the NtPPO inhibition results are shown in Tables 1 and 2.

Herbicidal Activity. Three representative broadleaf weeds *Abutilon juncea* (ABUJU), *Amaranthus retroflexus* (AMARE), and *Eclipta prostrata* (ECLPR) and three representative grass weeds *Digitaria sanguinalis* (DIGSA), *Echinochloa crus-galli* (ECHCG), and *Setaria faberi* (SETFA) were used to evaluate the post-emergent herbicidal activity the synthesized compounds **1a1** and **2−6**. The assay methods were the same as our previous reports.[29−32] Briefly, plastic pots (diameter of 7.5 cm) were filled with the clay soil to $^3/_4$ of their depth, then the seeds of the six kinds of weeds were sown in the pots and grown in the greenhouse. The test compounds were dissolved in dimethylformamide (DMF) and diluted with 0.1% Tween 80 solution before use. When the weeds grew to the three-leaf stage, they were treated by the tested compounds with the application rates of 37.5−150 g of ai/ha. The test solution (Tween 80 + DMF) and saflufenacil were used as blank and positive controls, respectively, with three replications for each compound and concentration. After 21 days post-treatment, the herbicidal activity of each compound was evaluated, and the results are illustrated in Tables 1 and 2.

Crop Safety. Six compounds **2a−2c** and **6a−6c** with a wide spectrum of weed control were selected for crop selectivity studies. Six representative crops, corn, rice, wheat, peanut, soybean, and cotton, were used in the crop safety experiments. The crop safety assay methods were similar to our previous reports.[11,24,25] Briefly, the seeds of the six kinds of crops were sown in plastic pots and grown in the greenhouse. When the tested crops reached the four-leaf stage, they were treated by compounds **2a−2c** and **6a−6c** at the rate of 150 g of ai/ha. Saflufenacil was used as a positive control, with three replicates for each compound. After 25 days, the crop damage (percent injury, %) of each compound was evaluated, and the results are shown in Table 3.

Stability Assay of Compounds 2c and 6c in the NtPPO Reaction Buffer. The assay method of compounds **2c** and **6c** in the NtPPO assay buffer was the same as our previous report.[11] Briefly, a reaction solution (400 μL) containing 200 μM compound **2c** or **6c**, assay buffer, NtPPO (20 μg), and protoporphyrinogen IX (1.8 μM) was incubated at room temperature for 3, 5, and 7 min, separately. Then, CH_3OH (135 μL) was added to the reaction solution. The remaining percentage of compounds **2c** and **6c** in the reaction buffer was then detected using high-performance liquid chromatography (HPLC, Agilent 1200 Infinity Series) with a C18 column (4.6 × 150 mm, 5.0 μm). For each compound, at least three repeats were performed.

Metabolism Studies of Compounds 2c and 6c in ABUJU. One of the tested weeds ABUJU was selected as the representative in the metabolism study.[11,24] Briefly, the five-leaf-stage ABUJU was treated by a solution of compound **2c** or **6c** (100 μM, containing 1‰ DMF and Tween 80) in the greenhouse. When the leaves of ABUJU started to drop (about 2−3 h), 5 g of the leaves was cut for further analysis. The leaves were first washed with a solution containing 1‰ DMF and Tween-80 3 times and then triturated to powder in the presence of liquid nitrogen. The powder was then transferred to a flask, which contained ethyl acetate (50 mL) and H_2O (100 mL), and stirred vigorously for 30 min at room temperature. The organic layer was separated and concentrated under reduced pressure. The residue was analyzed by UPLC−HRMS (Waters Acquity UPLC H-class, Waters Xevo G2-XS Q-TOF).

Molecular Docking. The structure of compounds **2c** and *R*- and *S*-**6c** were constructed and optimized by Sybyl 6.9 (Tripos, Inc.) before use. The crystal structure of NtPPO (PDB code 1SEZ) was download from the Protein Data Bank (PDB) database, and chain A of the structure was used for the subsequent molecular dynamic (MD) simulation studies. PYMOL was used to extract the receptor and visualized the simulation results.[33] AutoDockTools version 1.5.6 was used to prepare the ligands and receptors, and AutoDock 4.2 was used to predict the binding modes of compounds **2c** and *R*- and *S*-**6c** to NtPPO.[34] The docking parameters used in this research were the same as our previous reports.[11,24,25]

MD Simulations. AMBER 14 software package with ff14SB force fields was used to perform MD simulations of the **2c**− and (*R* and *S*) **6c**−NtPPO systems.[35] The parameters of ligands for MD simulations were prepared by the Antechamber program with the AMBER force fields (GAFF). The ligand−protein system was solvated with TIP3P

https://doi.org/10.1021/acs.jafc.1c00796
J. Agric. Food Chem. 2021, 69, 4081−4092

Scheme 1. Designed Synthetic Routes for Compound 1[a]

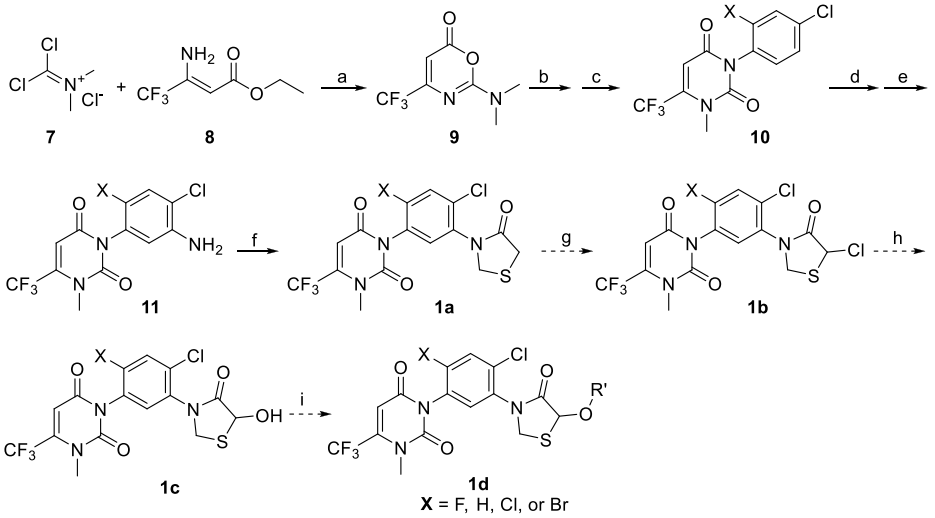

[a]Reagents and conditions: (a) $CHCl_3$, reflux; (b) 2-substituted 4-chloroaniline, acetic acid, reflux; (c) Cs_2CO_3, CH_3I, DMF, rt; (d) HNO_3, H_2SO_4, 0 °C−rt; (e) Fe, acetic acid (80%), 80 °C; (f) formaldehyde (37% in water), thioglycolic acid, *p*-toluenesulfonic acid, toluene, rt−reflux; (g) SO_2Cl_2, CH_2Cl_2, 0 °C; (h) K_2CO_3, H_2O, THF; and (i) R′I, THF, 0 °C.

water molecules in an 8.0 Å truncated octahedral box. Na^+ was used to neutralize the systems. First, the energy of each of the systems was minimized by the conjugate gradient and the steepest descent methods. Then, the systems were gently annealed from 0 to 300 K in 50 ps, followed by a 50 ps equilibrating calculation at 300 K and 1 atm using periodic boundary conditions in the *NPT* ensemble.[36] Finally, each of the systems was performed for 30 ns of MD simulation using the PMEMD module. The structures of the ligand−protein systems at 30 ns of the MD simulation were analyzed by the CPPTRAJ module. The last 10 ns of MD trajectories was used for the energy decomposition analysis and binding free energy calculation.

RESULTS AND DISCUSSION

Unexpected Discovery of *N*-Phenylaminomethylthioacetylpyrimidine-2,4-diones via Exploring the Reaction Intermediate of Compound 1a. To synthesize our initially designed *N*-phenyluracil thiazolidinone (**1**), we developed a linear synthetic route to prepare these compounds. As shown in Scheme 1, 2-(dimethylamino)-4-(trifluoromethyl)-6*H*-1,3-oxazin-6-one (**9**) was obtained in a yield of 86% by refluxing the reaction mixture of *N*-(dichloromethylene)-*N*-methylmethanaminium chloride (**7**) and ethyl-3-amino-4,4,4-trifluorobut-2-enoate (**8**) in $CHCl_3$. Then, intermediate **9** reacted with 2-substituted-4-chloroaniline to afford the corresponding *N*-phenyluracils; without further purification, the *N*-phenyluracils directly reacted with CH_3I using Cs_2CO_3 as a base to provide compound **10**. After the nitration and reduction reactions, intermediate **11** was obtained in yields of 82−89%. We hoped using an intramolecular ring closure reaction of compound **11**, formaldehyde, and thioglycolic acid could provide thiazolidinone derivative **1a**. Although we have made enormous efforts to synthesize compound **1a**, we still could not find a relatively efficient method to create compound **1a**. For example, we first tried to obtain compound **1a1** by refluxing a solution of compound **11a**, HCHO (37% in water), thioglycolic acid, and toluene for 12 or 24 h; however, no compound **1a1** was obtained (entries 1 and 2 in Table S1 of the Supporting Information). Next, we added the catalytic amount of *p*-toluenesulfonic acid (PTSA) to the reaction solution and used a Dean−Stark trap to remove H_2O in the reaction solution. After the reaction solution was heated to reflux for 12 h, compound **1a1** was obtained in only 16% yield (entry 3 in Table S1 of the Supporting Information). Additionally, we also observed that prolonging the reaction time did not improve the reaction yield (entry 4 in Table S1 of the Supporting Information). However, it was found that this reaction could not proceed at a large scale, because we only observed the trace amount of compound **1a1** when using 5 g of compound **11a** as the starting material (entry 5 in Table S1 of the Supporting Information). The low synthetic yield of compound **1a1** made it hard for subsequent transformations. Therefore, we made another round of optimization of reaction conditions to improve the synthetic yield of compound **11a** by varying the reaction solvent or temperature, while no improvements were observed (entries 6−9 in Table S1 of the Supporting Information).

After analysis of the reaction mechanism of synthesizing compound **1a1** using compound **11a** as the substrate, we proposed that compound **2a** might be the critical reaction intermediate in this ring-closure reaction (Scheme S1 of the Supporting Information). Therefore, we first synthesized compound **2a** by reacting compound **11a**, paraformaldehyde, and thioglycolic acid in toluene, and compound **2a** was obtained in a yield of 86% (Scheme S2 of the Supporting Information). Then, we hoped that compound **2a** could transform into compound **1a1** after undergoing an intramolecular dehydration reaction. We have tried various dehydration reagents, such as PTSA, boron trifluoride etherate, $FeCl_3$, and molecular sieves, to remove a water molecule from the structure of compound **2a**. Still, the yields were relatively low, with only a trace amount of compound **1a1** obtained. Besides, we also designed another alternative synthetic route to prepare compound **1a1**. As shown in Scheme S3 of the Supporting Information, compound **2b** could be efficiently synthesized by reacting amine **11a**, paraformaldehyde, and methyl thioglycolate in toluene. However, no conversion of compound **2b** to compound **1a1** was observed, even though various reaction conditions were screened (Table S2 of the

https://doi.org/10.1021/acs.jafc.1c00796
J. Agric. Food Chem. 2021, 69, 4081−4092

Supporting Information). Further attempts to synthesize compound **1a1** using similar reaction routes as that shown in Scheme S3 of the Supporting Information, by changing the methyl thioglycolate to ethyl mercaptoacetate, were proven unsuccessful as well.

As noted in the Introduction, the primary goal for us is to discover new compounds with improved bioactivity. However, substantial efforts by us have been invested in optimizing the reaction conditions of compound **1a1**, while little progress had been made. To surmount this dilemma, we intended to investigate the herbicidal activity and NtPPO inhibitory activity of compound **1a1** to check whether it deserved further optimization. Due to the fact that many PPO inhibitors have hydrophobic side chains in their structures.[14−16,37] Interestingly, the structures of our reaction intermediates **2a−2c** all have hydrophobic aminomethylthioacetyl groups. This observation inspired our curiosity to explore whether compounds **2a−2c** possessed good bioactivity. As illustrated in Table 1, the K_i value of compound **1a1** against NtPPO was 3.8 nM, showing a 2.6-fold improvement over saflufenacil (K_i = 10.0 nM). In addition, the PPO inhibitory activities of compounds **2a−2c** were 11.0, 28.6, and 11.0 nM, respectively, which were in the same order as saflufenacil. It is worth noting that, at the rate of 150 g of ai/ha, compound **1a1** showed excellent inhibition against four of the six tested weeds (ABUJU, AMARE, ECLPR, and DIGSA) and compounds **2a−2c** showed potent and excellent control (>80% inhibition) against all of the weeds tested. Further herbicidal activity evaluation indicated that all of compounds **2a−2c** exhibited broader and stronger activity than compound **1a1**, even at a low rate of 37.5 g of ai/ha. These unexpected findings indicated that compounds **2a−2c** could be used as a new scaffold for PPO inhibition, deserving further optimization. Therefore, a series of *N*-phenylaminomethylthioacetylpyrimidine-2,4-diones (**2−6**) were designed and synthesized.

Chemistry. As we have mentioned, compounds **2a−2c** could be efficiently synthesized by heating compound **11a** with paraformaldehyde and the corresponding thioglycolic acid derivatives in toluene, suggesting that other *N*-phenylaminomethylthioacetylpyrimidine-2,4-diones might also be constructed by this one-pot procedure. Next, the scope of this reaction was explored by varying the amine **11** and intermediate **12** (Scheme 2). As shown in Tables 1 and 2, wide

Scheme 2. Synthesis of Compounds 2−6[a]

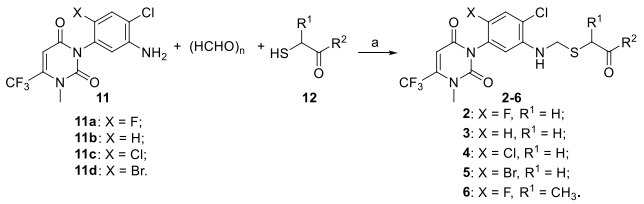

[a]Reagents and conditions: (a) toluene, rt−110 °C.

varieties of *N*-phenylaminomethylthioacetylpyrimidine-2,4-diones were smoothly prepared in good to excellent yields (48−95%). We also observed that different amines were well-tolerated in this one-pot reaction condition, providing the corresponding compounds **2d−2j**, **3**, **4**, and **5** in yields of 57−95, 84−92, 85−90, and 82−88%, respectively. The reaction procedure was also competent for the reaction of compound **11a** with 2-mercapto-*N*-substitutedacetamides, while the yields slightly dropped in comparison to that of compound **11a** reacting with thioglycolic acid derivatives. For example, the yields of compounds **2b−2e** were higher than those of compounds **2k−2m**. In addition, the 2-mercaptopropanoic acid derivatives reacted well with compound **11a** and paraformaldehyde, delivering the related products **6a−6i** in yields of 48−85%.

Additionally, attempts to oxidize the S atoms of compounds **2c** and **6c** using oxidation reagents did not provide the desired compounds (Tables S3 and S4 of the Supporting Information). We inferred that the reason might be that the aminomethylthioacetyl groups of compounds **2c** and **6c** were not stable under oxidation conditions. In the presence of oxidizing agents, the bonds between the *N*-phenylpyrimidine-2,4-dione moiety and side chains of compounds **2c** and **6c** could be easily cleaved.

Herbicidal Activity and Structure−Activity Relationship (SAR). As mentioned in the above section, the *N*-phenylaminomethylthioacetylpyrimidine-2,4-diones (**2a−2c**) were initially designed as the reaction intermediates to synthesize compound **1a1**, and unexpectedly, we observed that compounds **2a−2c** displayed higher herbicidal activity than compound **1a1**. Importantly, compounds **2a−2c** could be efficiently constructed by a one-pot synthetic approach. Encouraged by these promising findings, we explored the scope of this one-pot reaction and initiated a systematic SAR exploration of the synthesized compounds. As indicated in Tables 1 and 2, most of the compounds **2−6** exhibited strong herbicidal activity against six kinds of tested weeds at 150 g of ai/ha; some of them displayed excellent broadleaf weed control comparable to that of saflufenacil, even at 37.5 g of ai/ha.

To explore the SAR of *N*-phenylaminomethylthioacetylpyrimidine-2,4-diones, we first prepared a set of representative analogues around compounds **2a−2c** by varying the substituents at R^2. The results indicated that substituents at R^2 could affect the herbicidal spectrum of the target compounds (Table 1). For example, compounds **2a−2c** exhibited stronger herbicidal activity than their corresponding analogues **2k−2m** at 150 g of ai/ha; compound **2j** (R^2 = $-OCH_2CO_2C_2H_5$) displayed more than 85% control against the six tested weeds; and compound **2p** (R^2 = $-NHCH_2CO_2C_2H_5$) only showed mild herbicidal activity against the tested monocotyledon weeds at 150 g of ai/ha. After comparison of the *c* log *P* values of compounds **2k−2p** to their corresponding parent compounds, we observed that introducing the amino groups at R^2 would reduce the *c* log *P* values of the target molecules. Therefore, we proposed that substituting the amino groups at R^2 reduced the herbicidal spectrum by decreasing the absorption of compounds by weed leaves.[38,39] Additionally, it was found that prolonged side chains at R^2 failed to further improve the herbicidal potency of compound **2c**, because most compounds (**2d−2j**) showed moderate decreases in herbicidal activity. Interestingly, substituting $-NHCH_3$ of compound **2k** with longer chains (**2l−2q**) was found advantageous to broadleaf weed control.

Next, we explored the substituent effects on the herbicidal activity at the X position and synthesized compounds **3−5**. As illustrated in Table 1, changing the fluorine atoms to hydrogen atoms at the X position would markedly deteriorate the herbicidal potency, because all of the compound **3** exhibited decreased herbicidal activity relative to the corresponding fluorine substituted analogues **2a−2e**. In addition, replacing the hydrogen atoms with chlorine atoms, as in combination **4**,

https://doi.org/10.1021/acs.jafc.1c00796
J. Agric. Food Chem. 2021, 69, 4081−4092

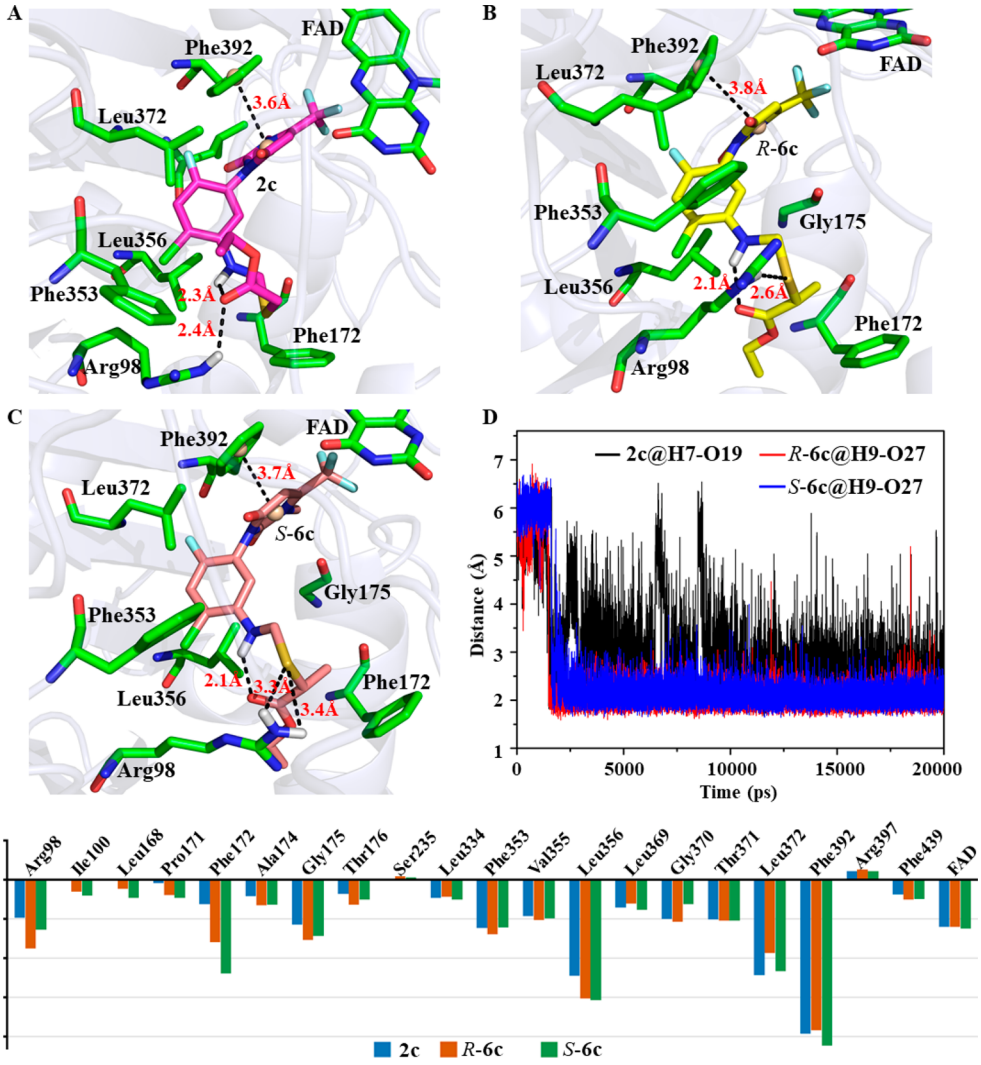

Figure 3. Molecular simulation studies of compounds **2c** and *R*- and *S*-**6c** with NtPPO. (A) Binding mode of the **2c**−NtPPO complex after 20 ns MD simulation; compound **2c** is shown as magenta sticks. (B) Binding mode of the *R*-**6c**−NtPPO complex after 20 ns MD simulation; compound *R*-**6c** is shown as yellow sticks. (C) Binding mode of the *S*-**6c**−NtPPO complex after 20 ns MD simulation; compound *S*-**6c** is shown as salmon sticks. (D) Distance analysis of **2c**@H7−O19, *R*-**6c**@H9−O27, and *S*-**6c**@H9−O27 during the MD simulation. (E) Comparison of the total interaction binding energies (kcal/mol) between compounds **2c** and *R*- and *S*-**6c** and NtPPO.

resulted in further decreases in herbicidal potency. Unfortunately, the replacement of chlorine atoms with bromine atoms (**5**) led to a significant loss in herbicidal potency. The above SAR results indicated that installing the fluorine atoms at the X position was found beneficial to herbicidal activity, while changing the fluorine atoms to hydrogen, chlorine, or bromine atoms was unfavorable (F > H > Cl > Br).

Finally, we fixed the X positon as a fluorine atom and introduced a methyl group at R^1 (**6**). The results indicated that, in most cases, replacement of the hydrogen atom with a methyl group at the position R^1 was found to have a slight improvement in herbicidal activity (Table 2). In particular, compound **6c** (R^1 = CH_3 and R^2 = $-OCH_2CH_3$) displayed excellent control (100%) against the tested broadleaf weeds and strong inhibition (>80%) against DIGSA, ECHCG, and SETFA, even as low as 37.5 g of ai/ha. After comparison of the *c* log *P* values of compound **6** to their corresponding mother molecules in compound series **2**, we inferred that substituting a methyl group at R^1 increased the herbicidal potency by improving the foliar uptake of the test compounds.[40]

Crop Selectivity. In an attempt to investigate whether some of the highly active *N*-phenylaminomethylthioacetylpyrimidine-2,4-diones could be used as herbicide leads for further development or not, we tested the post-emergence crop selectivity of six representative compounds **2a**−**2c** and **6a**−**6c** against corn, rice, wheat, soybean, cotton, and peanut. As illustrated in Table 3, at the rate of 150 g of ai/ha, compounds **2a** and **2c** were selective in rice and compound **2b** exhibited high crop safety for wheat, whereas compounds **6a**−**6c** showed limited crop safety (crop injury of >10%) toward the six tested crops. However, even at a relatively lower rate of 75 g of ai/ha, saflufenacil still exhibited high crop damage to the six tested crops. Together, our results revealed that installing a methyl group at R^1 would reduce crop safety. Thus, compound **2c** was found to be the most promising lead compound for weed control in paddy fields.

PPO Inhibition Activity. As shown in Tables 1 and 2, most compounds with high levels of weed control at 37.5−150 g of ai/ha also exhibited strong NtPPO inhibitory activity. For example, compound **2d**, with a K_i value of 17.4 nM, displayed

https://doi.org/10.1021/acs.jafc.1c00796
J. Agric. Food Chem. 2021, 69, 4081−4092

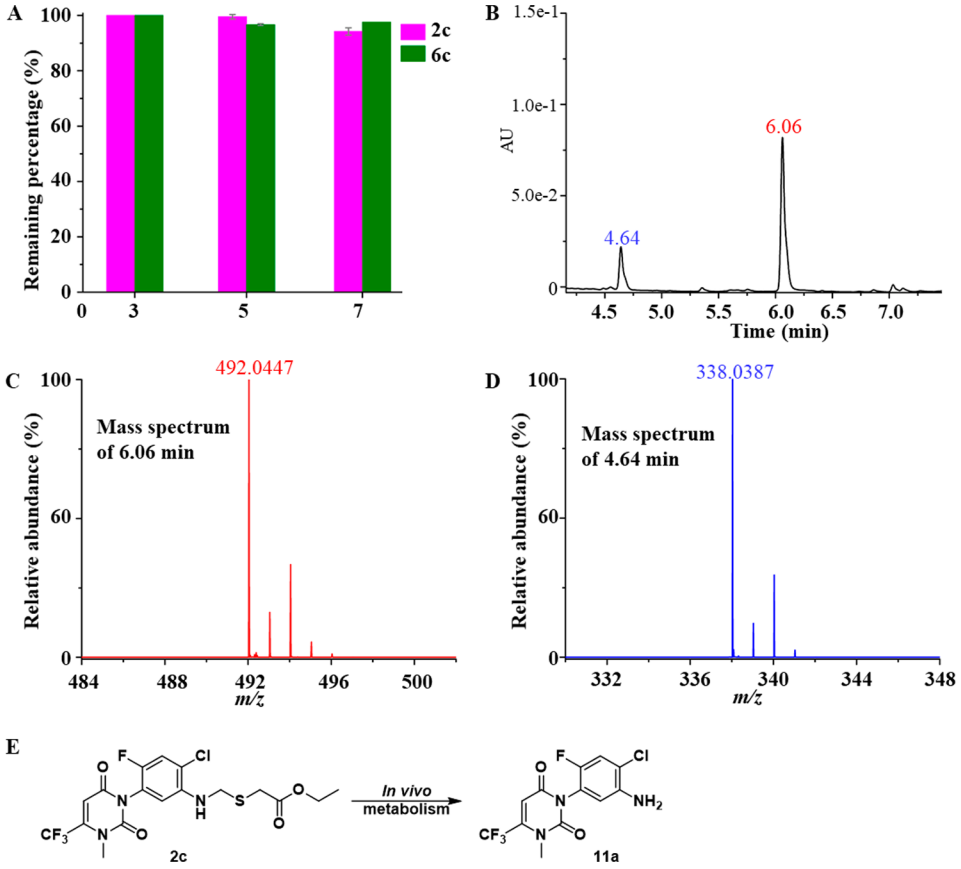

Figure 4. Stability and metabolism studies of compound **2c**. (A) Stability studies of compounds **2c** and **6c** in NtPPO assay solutions for different times; each experiment was repeated 3 times; and the error bar was shown as the standard error. (B) UPLC analyzed the leaf extract of ABUJU after treating by compound **2c** for 3 h. (C) HRMS spectrum of the peak at 6.06 min, and the spectrum corresponded to compound **2c**. (D) HRMS spectrum of the peak at 4.64 min, and this spectrum corresponded to compound **11a**. (E) Proposed metabolism pathway of compound **2c** *in planta*. In this pathway, compound **2c** was deactivated by hydrolyzing to amino intermediate **11a**.

100% control against the six tested weeds at 150 g of ai/ha; compound **2j** (K_i = 4.4 nM) exhibited excellent weed control at 150 g of ai/ha; and compound **6c** (K_i = 2.3 nM) showed excellent weed control at 37.5−75 g of ai/ha. It was observed that, for compounds with different substituents at the X position, the fluorine-containing analogue **2** showed higher inhibition potency than the hydrogen-, chloro-, and bromo-substituted analogues **3**, **4**, and **5**, respectively (F > H > Cl > Br). The same SAR trend has also been found in the herbicidal activity assay of these analogues. Additionally, we found that, in most cases, the NtPPO inhibitory potency improved with increasing the side-chain length of R^2. One such example was that of compound **2m** (R^2 = $-NHCH_2CH_2CH_3$; K_i = 3.0 nM), showing slightly higher inhibitory potency relative to compound **2l** (R^2 = $-NHCH_2CH_3$; K_i = 3.6 nM) and compound **2k** (R^2 = $-NHCH_3$; K_i = 27.1 nM). Besides, for most compounds in series **2**, placing a methyl group at R^1 was found favorable to PPO inhibitory activity as well, such as compound **6c** (R^1 = $-CH_3$; K_i = 2.3 nM) exhibiting improved inhibition potency compared to compound **2c** (R^1 = H; K_i = 11.0 nM) and compound **6h** (R^1 = $-CH_3$; K_i = 8.5 nM) displaying higher activity than that of compound **2p** (R^1 = H; K_i = 15.3 nM).

Molecular Simulation Studies. To obtain deeper insight into the inhibition mechanism of the newly synthesized compounds **2**−**6**, two representative compounds **2c** and **6c** were selected for the subsequent molecular simulation studies. Because there is a chiral center of compound **6c**, we studied the binding mechanisms of both *R* and *S* configurations of compound **6c**. First, we docked compounds **2c** and *R*- and *S*-**6c** to the catalytic pocket of NtPPO (PDB code 1SEZ) using AutoDock 4.2 software.[23,34] The best binding modes of the three compounds were selected on the basis of binding sores and the reference ligand in the crystal structure. Then, we performed a 20 ns MD simulation of each of the **2c**−, *R*-**6c**−, and *S*-**6c**−NtPPO systems to reveal the inhibition mechanisms of compounds **2c** and **6c** (Figure S1 of the Supporting Information). As shown in Table S5 of the Supporting Information, the ΔE_{ele} values of **2c**−, *R*-**6c**−, and *S*-**6c**−NtPPO systems were −22.45, −24.94, and −23.80 kcal/mol, respectively, suggesting that the electrostatic energies, such as the hydrogen-bonding interactions of the three compounds, might be the same, whereas the ΔE_{vdw} values of compounds *R*-**6c** (−64.65 kcal/mol) and *S*-**6c** (−63.33 kcal/mol) with NtPPO were higher than that of compound **2c** (−54.12 kcal/mol), which, in turn, resulted in improved binding free energies of compounds *R*- and *S*-**6c** compared to compound **2c**. The binding free energies (ΔG_{bind}) of compounds **2c** and *R*- and *S*-**6c** with NtPPO were −24.89, −29.57, and −33.87 kcal/mol, suggesting that compound **6c** bonded more tightly to NtPPO than compound **2c**, which showed the same trend as the NtPPO inhibition experiments.

To better understand the crucial structural features of the binding mode between compound **2c** or *R*- or *S*-**6c** and

https://doi.org/10.1021/acs.jafc.1c00796
J. Agric. Food Chem. 2021, 69, 4081−4092

NtPPO, we analyzed the binding modes of the **2c**− and *R*- and *S*-**6c**−NtPPO systems at 20 ns (panels A−C of Figure 3). The results indicated that there were no significant differences in the binding modes of the three compounds with NtPPO, and the key interactions on the binding surface were highly conservative, for example, the favorable $\pi-\pi$ interaction of the uracil ring with Phe392, the conserved hydrophobic interactions of the benzene ring with Leu372 and Leu356, T-shaped $\pi-\pi$ stacking interaction of Phe353 with the benzene ring, and hydrophobic interactions of Phe172 with the side chains of the three compounds. We also observed that, in the **2c**−NtPPO system, the terminal carboxyl group of compound **2c** could form a hydrogen-bonding interaction with Arg98 (Figure 3A). In contrast to compound **2c**, the sulfur atoms of compounds *R*- and *S*-**6c** could form N−H···S hydrogen-bonding interactions with Arg98 (panels B and C of Figure 3).[41]

Interestingly, we found that, after MD simulations, the side chains of the three compounds adopted a twisted orientation and formed seven-membered rings. The rings were furtherly stabilized through the favorable intramolecular hydrogen-bond interaction between the NH group and the carbonyl group of the side chains (panels A−C of Figure 3). However, the formation of seven-membered rings was not observed after docking studies (Figure S2 of the Supporting Information). For the sake of clarity, we defined the hydrogen bond between the NH group and the carbonyl group of the side chains of compounds **2c** and *R*- and *S*-**6c** as **2c**@H7−O19, *R*-**6c**@H9−O27, and *S*-**6c**@H9−O27, respectively. Further analysis indicated that, after 2 ns MD simulations, the distances of *R*- and *S*-**6c**@H9−O27 had reached around 2.1 Å, while it took about 10 ns for **2c**@H7−O19 to reach equilibration, and the final distance of **2c**@H7−O19 was around 2.8 Å (Figure 3D), suggesting that the seven-membered rings of compounds *R*- and *S*-**6c** were more stable that of compound **2c**. Additionally, the results of energy decomposition studies of the **2c**− and *R*- and *S*-**6c**−NtPPO systems indicated that forming a more stable seven-membered ring system could improve the energy contribution of Phe172, because the energy contributions of Phe172 of *R*-**6c**−NtPPO (−1.60 kcal/mol) and *S*-**6c**−NtPPO (−2.39 kcal/mol) were higher than that of **2c**−NtPPO (−0.62 kcal/mol) (Figure 3E). Together, our results suggested that installing a methyl group at R^1 could induce the formation of a more stable seven-membered ring system of the target molecule, which, in turn, caused a strong synergistic effect in improving the π-alkyl interaction between Phe172 and the molecule.

Stability and Metabolism Studies. Because there are aminomethylthioacetyl groups in the structures of compounds **2c** and **6c**, to understand whether compounds **2c** and **6c** are stable *in vitro* or not, we tested the stability of compounds **2c** and **6c** in the PPO activity assay buffer using the HPLC assay. As shown in Figure 4A, almost no hydrolysis was observed after compounds **2c** and **6c** were incubated in PPO activity assay solution for 3 min. After 5 min of incubation, the degradation percentage of compound **2c** was still less than 0.5%, while about 3% of compound **6c** was decomposed. Even after a relatively long incubation time, both compounds **2c** and **6c** still showed a very slight degree of degradation. As a result of the character of NtPPO and the substrate protoporphyrinogen IX, a linear increase in fluorescence usually occurred within 3 or 5 min. Simultaneously, the limited degradation of compounds **2c** and **6c** almost did not affect their inhibitory potency.

Additionally, we also investigated the metabolism of compounds **2c** and **6c** *in planta* using the UPLC−HRMS assay. ABUJU was selected as the representative weed for the metabolism study. The results indicate that, when the leaves of ABUJU started to drop, there was still compounds **2c** and **6c** in the plants because the retention time at 6.06 min (Figure 4B) and mass peak at 492.0447 (Figure 4C) corresponded to compound **2c** and the retention time at 6.41 min (Figure S3A of the Supporting Information) and mass peak at 506.0683 (Figure S3B of the Supporting Information) corresponded to compound **6c**. After a careful analysis of the UPLC−HRMS results, we found a metabolite with the retention time at 4.64 min and mass peak at 338.0387 (Figure 4D and Figure S3C of the Supporting Information) existed in both the **2c**- and **6c**-treated samples. According to the chemical properties of compounds **2c** and **6c**, we inferred that the metabolite was compound **11a** based on the molecular weight. Meanwhile, we also found that, in the **2c**-treated sample, about 20% of compound **2c** was degraded to compound **11a**, while only 10% of compound **6c** was metabolized to compound **11a**. These results suggest that both compounds **2c** and **6a** are prone to metabolize by cleaving the NH bridge between the phenyluracil moiety and the methylthioacetyl group side chains (Figure 4E and Figure S3C of the Supporting Information). In comparison, the metabolism rate of compound **2c** was 2-fold faster than that of compound **6c**.

In conclusion, we described the unexpected discovery of a novel series of *N*-phenylaminomethylthioacetylpyrimidine-2,4-diones (**2**−**6**) as potent PPO inhibitors by taking advantage of the reaction intermediates of our initially designed *N*-phenyluracil thiazolidinone (**1**). A total of 41 of the newly generated compounds **2**−**6** were prepared by an efficient one-pot procedure in good to excellent yields. Systematic NtPPO inhibition and herbicidal activity evaluations were performed on the target compounds. The results revealed that some compounds showed improved NtPPO inhibition potency compared to saflufenacil and excellent herbicidal activity at 37.5−150 g of ai/ha. Promisingly, compound **2c**, with a K_i value of 11 nm, not only exhibited excellent weed control at 37.5−150 g of ai/ha but also showed high crop safety toward rice at 150 g of ai/ha. Our molecular simulation studies revealed that the side chains of compound **2c** could form a hydrogen-bond-mediated seven-membered ring system. Installing a methyl group at R^1 could reinforce the hydrogen bond of the ring system, which, in turn, increased the binding affinity of the target molecule. Furthermore, we found that, *in planta*, compound **2c** was deactivated by hydrolyzing to compound **11a**, while introducing a methyl group at R^1 could reduce the metabolic rate and improve the bioactivity. Taken together, our study provides new insights into the discovery of novel PPO inhibitors through exploring the reaction intermediate approach.

■ ASSOCIATED CONTENT

Supporting Information

The Supporting Information is available free of charge at https://pubs.acs.org/doi/10.1021/acs.jafc.1c00796.

Synthetic details, NMR and HRMS characterization data of compounds **2b**−**2q** and **3**−**6**, reaction condition optimization for compound **1a1** (Tables S1 and S2,

https://doi.org/10.1021/acs.jafc.1c00796
J. Agric. Food Chem. 2021, 69, 4081−4092

optimization of the reaction conditions for compounds **2c1** and **6c1** (Table S3), optimization of the reaction conditions for compounds **2c2** and **6c2** (Table S4), predicted binding free energies of compounds **2** and *R*- and *S*-**6c** with NtPPO (Table S5), synthetic routes for compound **1a1** (Schemes S1−S3), RMSD analysis of **2c**− and *R*- and *S*-**6c**−NtPPO systems (Figure S1), predicted binding modes of compounds **2c** and *R*- and *S*-**6c** with NtPPO by AutoDock 4.2 software (Figure S2), and metabolism studies of compound **6c** (Figure S3) (PDF)

AUTHOR INFORMATION

Corresponding Author

Zhen Xi − *State Key Laboratory of Elemento-Organic Chemistry and Department of Chemical Biology, National Pesticide Engineering Research Center, Collaborative Innovation Center of Chemical Science and Engineering, College of Chemistry, Nankai University, Tianjin 300071, People's Republic of China;* orcid.org/0000-0002-3332-5413; Phone: +86-022-23504782; Email: zhenxi@nankai.edu.cn

Authors

Da-Wei Wang − *State Key Laboratory of Elemento-Organic Chemistry and Department of Chemical Biology, National Pesticide Engineering Research Center, Collaborative Innovation Center of Chemical Science and Engineering, College of Chemistry, Nankai University, Tianjin 300071, People's Republic of China*

Lu Liang − *State Key Laboratory of Elemento-Organic Chemistry and Department of Chemical Biology, National Pesticide Engineering Research Center, Collaborative Innovation Center of Chemical Science and Engineering, College of Chemistry, Nankai University, Tianjin 300071, People's Republic of China*

Zhi-Yuan Xue − *State Key Laboratory of Elemento-Organic Chemistry and Department of Chemical Biology, National Pesticide Engineering Research Center, Collaborative Innovation Center of Chemical Science and Engineering, College of Chemistry, Nankai University, Tianjin 300071, People's Republic of China*

Shu-Yi Yu − *State Key Laboratory of Elemento-Organic Chemistry and Department of Chemical Biology, National Pesticide Engineering Research Center, Collaborative Innovation Center of Chemical Science and Engineering, College of Chemistry, Nankai University, Tianjin 300071, People's Republic of China*

Rui-Bo Zhang − *State Key Laboratory of Elemento-Organic Chemistry and Department of Chemical Biology, National Pesticide Engineering Research Center, Collaborative Innovation Center of Chemical Science and Engineering, College of Chemistry, Nankai University, Tianjin 300071, People's Republic of China*

Xia Wang − *State Key Laboratory of Elemento-Organic Chemistry and Department of Chemical Biology, National Pesticide Engineering Research Center, Collaborative Innovation Center of Chemical Science and Engineering, College of Chemistry, Nankai University, Tianjin 300071, People's Republic of China*

Han Xu − *State Key Laboratory of Elemento-Organic Chemistry and Department of Chemical Biology, National Pesticide Engineering Research Center, Collaborative Innovation Center of Chemical Science and Engineering, College of Chemistry, Nankai University, Tianjin 300071, People's Republic of China*

Xin Wen − *State Key Laboratory of Elemento-Organic Chemistry and Department of Chemical Biology, National Pesticide Engineering Research Center, Collaborative Innovation Center of Chemical Science and Engineering, College of Chemistry, Nankai University, Tianjin 300071, People's Republic of China*

Complete contact information is available at: https://pubs.acs.org/10.1021/acs.jafc.1c00796

Funding

This research was funded in part by the National Key Research and Development Program of China (2017YFD0200501) and the National Natural Science Foundation of China (21837001 and 21702111).

Notes

The authors declare no competing financial interest.

REFERENCES

(1) Ahrens, H.; Lange, G.; Müller, T.; Rosinger, C.; Willms, L.; Van Almsick, A. 4-Hydroxyphenylpyruvate dioxygenase inhibitors in combination with safeners: Solutions for modern and sustainable agriculture. *Angew. Chem., Int. Ed.* **2013**, *52*, 9388−9398.

(2) Dayan, F. E. Current status and future prospects in herbicide discovery. *Plants* **2019**, *8*, 341.

(3) Yoon, J.; Han, Y.; Ahn, Y. O.; Hong, M. K.; Sung, S. K. Characterization of HemY-type protoporphyrinogen IX oxidase genes from cyanobacteria and their functioning in transgenic Arabidopsis. *Plant Mol. Biol.* **2019**, *101*, 561−574.

(4) Patzoldt, W. L.; Hager, A. G.; McCormick, J. S.; Tranel, P. J. A codon deletion confers resistance to herbicides inhibiting protoporphyrinogen oxidase. *Proc. Natl. Acad. Sci. U. S. A.* **2006**, *103*, 12329−12334.

(5) Chen, X. M.; Pu, H.; Fang, Y.; Wang, X.; Zhao, S.; Lin, Y.; Zhang, M.; Dai, H. E.; Gong, W. M.; Liu, L. Crystal structure of the catalytic subunit of magnesium chelatase. *Nat. Plants* **2015**, *1*, 15125.

(6) Rhee, H. W.; Zou, P.; Udeshi, N. D.; Martell, J. D.; Mootha, V. K.; Carr, S. A.; Ting, A. Y. Proteomic mapping of mitochondria in living cells via spatially restricted enzymatic tagging. *Science* **2013**, *339*, 1328−1331.

(7) Wang, B. F.; Wen, X.; Qin, X. H.; Wang, Z. F.; Tan, Y.; Shen, Y. Q.; Xi, Z. Quantitative structural insight into human variegate porphyria disease. *J. Biol. Chem.* **2013**, *288*, 11731−11740.

(8) Horn, P. J. Where do the electrons go? How numerous redox processes drive phytochemical diversity. *Phytochem. Rev.* **2021**, DOI: 10.1007/s11101-020-09738-w.

(9) Wang, B. F.; Wen, X.; Xi, Z. Molecular simulations bring new insights into protoporphyrinogen IX oxidase/protoporphyrinogen IX interaction modes. *Mol. Inf.* **2016**, *35*, 476−482.

(10) Hao, G. F.; Zuo, Y.; Yang, S. G.; Yang, G. F. Protoporphyrinogen oxidase inhibitor: An ideal target for herbicide discovery. *Chimia* **2011**, *65*, 961−969.

(11) Zhang, R. B.; Yu, S. Y.; Liang, L.; Ismail, I.; Wang, D. W.; Li, Y. H.; Xu, H.; Wen, X.; Xi, Z. Design, synthesis, and molecular mechanism studies of *N*-Phenylisoxazoline-thiadiazolo[3,4-*a*]-pyridazine hybrids as protoporphyrinogen IX oxidase inhibitors. *J. Agric. Food Chem.* **2020**, *68*, 13672−13684.

(12) Umetsu, N.; Shirai, Y. Development of novel pesticides in the 21st century. *J. Pestic. Sci.* **2020**, *45*, 54−74.

(13) Theodoridis, G.; Bahr, J. T.; Hotzman, F. W.; Sehgel, S.; Suarez, D. P. New generation of protox-inhibiting herbicides. *Crop Prot.* **2000**, *19*, 533−535.

(14) Park, J.; Ahn, Y. O.; Nam, J. W.; Hong, M. K.; Song, N.; Kim, T.; Yu, G. H.; Sung, S. K. Biochemical and physiological mode of

action of tiafenacil, a new protoporphyrinogen IX oxidase-inhibiting herbicide. *Pestic. Biochem. Physiol.* **2018**, *152*, 38−44.
(15) Zuo, Y.; Wu, Q.; Su, S. W.; Niu, C. W.; Xi, Z.; Yang, G. F. Synthesis, herbicidal activity, and QSAR of novel *N*-benzothiazolylpyrimidine-2,4-diones as protoporphyrinogen oxidase inhibitors. *J. Agric. Food Chem.* **2016**, *64*, 552−562.
(16) Yang, J.; Guan, A.; Wu, Q.; Cui, D.; Liu, C. Design, synthesis and herbicidal evaluation of novel uracil derivatives containing an isoxazoline moiety. *Pest Manage. Sci.* **2020**, *76*, 3395−3402.
(17) Cascioferro, S.; Parrino, B.; Carbone, D.; Schillaci, D.; Giovannetti, E.; Cirrincione, G.; Diana, P. Thiazoles, their benzofused systems, and thiazolidinone derivatives: Versatile and promising tools to combat antibiotic resistance. *J. Med. Chem.* **2020**, *63*, 7923−7956.
(18) Suryawanshi, R.; Jadhav, S.; Makwana, N.; Desai, D.; Chaturbhuj, D.; Sonawani, A.; Idicula-Thomas, S.; Murugesan, V.; Katti, S. B.; Tripathy, S.; Paranjape, R.; Kulkarni, S. Evaluation of 4-thiazolidinone derivatives as potential reverse transcriptase inhibitors against HIV-1 drug resistant strains. *Bioorg. Chem.* **2017**, *71*, 211−218.
(19) de Siqueira, L. R. P.; de Moraes Gomes, P. A. T.; de Lima Ferreira, L. P.; de Melo Rego, M. J. B.; Leite, A. C. L. Multi-target compounds acting in cancer progression: Focus on thiosemicarbazone, thiazole and thiazolidinone analogues. *Eur. J. Med. Chem.* **2019**, *170*, 237−260.
(20) Mitchell, G.; Barnes, N. J.; Cox, J. M.; Matthews, I. R.; Parry, D. R.; Pearson, D. P. J.; Smith, S. C. Synthesis and structure-activity relationships in a novel class of *N*-aryl lactam herbicides. In *Synthesis and Chemistry of Agrochemicals VI*; Baker, D. R., Fenyes, J. G., Lahm, G. P., Selby, T. P., Stevenson, T. M., Eds.; American Chemical Society (ACS): Washington, D.C., 2001; ACS Symposium Series, Vol. *800*, Chapter 3, pp 18−29, DOI: 10.1021/bk-2002-0800.ch003.
(21) Hao, G. F.; Zuo, Y.; Yang, S. G.; Chen, Q.; Zhang, Y.; Yin, C. Y.; Niu, C. W.; Xi, Z.; Yang, G. F. Computational discovery of potent and bioselective protoporphyrinogen IX oxidase inhibitor via fragment deconstruction analysis. *J. Agric. Food Chem.* **2017**, *65*, 5581−5588.
(22) Zhao, L. X.; Jiang, M. J.; Hu, J. J.; Zou, Y. L.; Cheng, Y.; Ren, T.; Gao, S.; Fu, Y.; Ye, F. Design, synthesis, and herbicidal activity of novel diphenyl ether derivatives containing fast degrading tetrahydrophthalimide. *J. Agric. Food Chem.* **2020**, *68*, 3729−3741.
(23) Koch, M.; Breithaupt, C.; Kiefersauer, R.; Freigang, J.; Huber, R.; Messerschmidt, A. Crystal structure of protoporphyrinogen IX oxidase: A key enzyme in haem and chlorophyll biosynthesis. *EMBO J.* **2004**, *23*, 1720−1728.
(24) Wang, D. W.; Zhang, R. B.; Yu, S. Y.; Liang, L.; Ismail, I.; Li, Y. H.; Xu, H.; Wen, X.; Xi, Z. Discovery of novel *N*-isoxazolinylphenyltriazinones as promising protoporphyrinogen IX oxidase inhibitors. *J. Agric. Food Chem.* **2019**, *67*, 12382−12392.
(25) Wang, D. W.; Zhang, R. B.; Ismail, I.; Xue, Z. Y.; Liang, L.; Yu, S. Y.; Wen, X.; Xi, Z. Design, herbicidal activity, and QSAR analysis of cycloalka[*d*]quinazoline-2,4-dione-benzoxazinones as protoporphyrinogen IX oxidase inhibitors. *J. Agric. Food Chem.* **2019**, *67*, 9254−9264.
(26) Wang, D. W.; Li, Q.; Wen, K.; Ismail, I.; Liu, D. D.; Niu, C. W.; Wen, X.; Yang, G. F.; Xi, Z. Synthesis and herbicidal activity of pyrido[2,3-*d*]pyrimidine-2,4-dione-benzoxazinone hybrids as protoporphyrinogen oxidase inhibitors. *J. Agric. Food Chem.* **2017**, *65*, 5278−5286.
(27) Hao, G. F.; Tan, Y.; Xu, W. F.; Cao, R. J.; Xi, Z.; Yang, G. F. Understanding resistance mechanism of protoporphyrinogen oxidase-inhibiting herbicides: Insights from computational mutation scanning and site-directed mutagenesis. *J. Agric. Food Chem.* **2014**, *62*, 7209−7215.
(28) Shepherd, M.; Dailey, H. A. A continuous fluorimetric assay for protoporphyrinogen oxidase by monitoring porphyrin accumulation. *Anal. Biochem.* **2005**, *344*, 115−121.
(29) Wang, D. W.; Lin, H. Y.; Cao, R. J.; Ming, Z. Z.; Chen, T.; Hao, G. F.; Yang, W. C.; Yang, G. F. Design, synthesis and herbicidal activity of novel quinazoline-2,4-diones as 4-hydroxyphenylpyruvate dioxygenase inhibitors. *Pest Manage. Sci.* **2015**, *71*, 1122−1132.
(30) Wang, D. W.; Lin, H. Y.; He, B.; Wu, F. X.; Chen, T.; Chen, Q.; Yang, W. C.; Yang, G. F. An efficient one-pot synthesis of 2-(aryloxyacetyl)cyclohexane-1,3-diones as herbicidal 4-hydroxyphenylpyruvate dioxygenase inhibitors. *J. Agric. Food Chem.* **2016**, *64*, 8986−8993.
(31) Wang, D. W.; Lin, H. Y.; Cao, R. J.; Yang, S. G.; Chen, Q.; Hao, G. F.; Yang, W. C.; Yang, G. F. Synthesis and herbicidal evaluation of triketone-containing quinazoline-2,4-diones. *J. Agric. Food Chem.* **2014**, *62*, 11786−11796.
(32) Wang, D. W.; Lin, H. Y.; Cao, R. J.; Chen, T.; Wu, F. X.; Hao, G. F.; Chen, Q.; Yang, W. C.; Yang, G. F. Synthesis and herbicidal activity of triketone-quinoline hybrids as novel 4-hydroxyphenylpyruvate dioxygenase inhibitors. *J. Agric. Food Chem.* **2015**, *63*, 5587−5596.
(33) DeLano, W. L. *The PyMOL Molecular Graphics System*; Delano Scientific: San Carlos, CA, 2002.
(34) Morris, G. M.; Huey, R.; Lindstrom, W.; Sanner, M. F.; Belew, R. K.; Goodsell, D. S.; Olson, A. J. AutoDock4 and AutoDockTools4: Automated docking with selective receptor flexibility. *J. Comput. Chem.* **2009**, *30*, 2785−2791.
(35) Case, D. A.; Babin, V.; Berryman, J. T.; Betz, R. M.; Cai, Q.; Cerutti, D. S.; Cheatham, T. E., III; Darden, T. A.; Duke, R. E.; Gohlke, H.; Goetz, A. W.; Gusarov, S.; Homeyer, N.; Janowski, P.; Kaus, J.; Kolossváry, I.; Kovalenko, A.; Lee, T. S.; LeGrand, S.; Luchko, T.; Luo, R.; Madej, B.; Merz, K. M.; Paesani, F.; Roe, D. R.; Roitberg, A.; Sagui, C.; Salomon-Ferrer, R.; Seabra, G.; Simmerling, C. L.; Smith, W.; Swails, J.; Walker, R. C.; Wang, J.; Wolf, R. M.; Wu, X.; Kollman, P. A. *AMBER 14*; University of California, San Francisco: San Francisco, CA, 2014.
(36) Yang, J.-F.; Yin, C.-Y.; Wang, D.; Jia, C.-Y.; Hao, G.-F.; Yang, G.-F. Molecular determinants elucidate the selectivity in abscisic acid receptor and HAB1 protein interactions. *Front. Chem.* **2020**, *8*, 425.
(37) Jiang, L. L.; Zuo, Y.; Wang, Z. F.; Tan, Y.; Wu, Q. Y.; Xi, Z.; Yang, G. F. Design and syntheses of novel *N*-(benzothiazol-5-yl)-4,5,6,7-tetrahydro-1*H*-isoindole-1,3(2*H*)-dione and *N*-(benzothiazol-5-yl)isoindoline-1,3-dione as potent protoporphyrinogen oxidase inhibitors. *J. Agric. Food Chem.* **2011**, *59*, 6172−6179.
(38) Avram, S.; Funar-Timofei, S.; Borota, A.; Chennamaneni, S. R.; Manchala, A. K.; Muresan, S. Quantitative estimation of pesticide-likeness for agrochemical discovery. *J. Cheminf.* **2014**, *6*, 42.
(39) Hao, G. F.; Dong, Q. J.; Yang, G. F. A comparative study on the constitutive properties of marketed pesticides. *Mol. Inf.* **2011**, *30*, 614−622.
(40) Wu, J. W.; Hsieh, C. L.; Wang, H. Y.; Chen, H. Y. Inhibitory effects of guava (*Psidium guajava* L.) leaf extracts and its active compounds on the glycation process of protein. *Food Chem.* **2009**, *113*, 78−84.
(41) Biswal, H. S.; Wategaonkar, S. Nature of the N−H···S Hydrogen Bond. *J. Phys. Chem. A* **2009**, *113*, 12763−12773.

https://doi.org/10.1021/acs.jafc.1c00796
J. Agric. Food Chem. 2021, 69, 4081−4092